BORE JEGDIĆ[1], BILJANA BOBIĆ[1], BOJAN GLIGORIJEVIĆ[2],
VESNA MIŠKOVIĆ-STANKOVIĆ[3]

Corrosion properties of an aluminium alloy 7000 series after a new two step precipitation hardening

Corrosion properties of an aluminium alloy 7000 series were investigated by different electrochemical methods. The alloy was subjected to the one-step and to a new two-step precipitation hardening. Polarization measurements in the 3.5 wt. % NaCl solution have shown a more positive value of the pitting potential (E_{pit}) and a higher corrosion resistance for the two-step aged alloy. The electrochemical impedance spectroscopy (EIS) has also shown that the two-step aged alloy has better corrosion properties (higher value of polarization resistance, R_p, and lower value of double-layer capacitance, C_{dl}) comparing to the one-step aged alloy.
Keywords: aluminium alloys, precipitation hardening, corrosion, electrochemical methods.

1. INTRODUCTION

Aluminium alloys of 7000 series (Al-Zn-Mg-Cu) are distinguished with maximum strength of all aluminium alloys. However, they are prone to localized corrosion forms and especially to stress corrosion cracking (SCC). The tendency of these alloys towards localized forms of corrosion depends on the content of alloying elements as well as on mechanical, thermal and thermo-mechanical treatments [1-3]. The precipitation hardening of the 7000 series aluminium alloys has been achieved by the segregation of GP zones that are transformed through the intermediate η' phase into the equilibrium phase $MgZn_2$ [4-7]. The maximum strength of the alloys has been obtained in the presence of a mixture of GP zones and η' precipitates in the structure. In the state of maximum strength, the 7000 series alloys are prone to SCC and exfoliation corrosion. In the over-aged state, these alloys are characterized with a good resistance towards both types of corrosion. In the partially over-aged state, the alloys show a slightly lower resistance to SCC and high resistance to exfoliation corrosion [4, 6, 8, 9].

The presence of copper in the 7000 series aluminium alloys has a beneficial effect on hardness, due to an increase in the volume fraction of hardening precipitates. It has been found that copper is

incorporated in GP zones, making them more stable even at higher temperatures [4, 10]. Also, copper atoms replace zinc atoms in the hardening precipitate η' ($MgZn_2$), particularly at temperatures above 150 °C [10], making the precipitate nobler. All this provide conditions for the increased resistance of the 7000 series aluminium alloys to localised forms of corrosion.

In the over-aged state, achieved by standard two-step aging, the 7000 series aluminium alloys exhibited high resistance to exfoliation corrosion and SCC [3-5]. However, the aging time is relatively long, and the hardness of the alloys is significantly reduced (15 % compared to the state of maximum hardness). A new two-step aging process was proposed, based on the reported results [11,12]. This aging process can be performed for a significantly shorter time. Tensile properties of the tested alloy after the new two-step aging remain unchanged compared to the alloy in the state of maximum hardness. The alloy after the new two-step aging process exhibited high resistance to SCC [13].

The composition of the solid solution, formed during aging process, has the greatest influence on the corrosion behaviour of an aluminium alloy [9]. Electrochemical and corrosion characteristics of the experimental aluminium alloy of maximum hardness, as well as in the state after the new two-step aging, were investigated in this study.

Author's address: [1]Institute for Chemistry, Technology and Metallurgy, University of Belgrade, Njegoseva 12, Belgrade, [2]Innovation center, Faculty of Technology and Metallurgy, University of Belgrade, Karnegieva 4, Belgrade, [3]Faculty of Technology and Metallurgy, University of Belgrade, Karnegijeva 4, Belgrade, Serbia

2. EXPERIMENTAL PART

2.1. Material and heat treatment

Chemical composition of the experimental aluminium alloy is given in Table 1.

Table 1 - Chemical composition of tested aluminium alloy (wt. %)

Zn	Mg	Cu	Mn	Cr	Zr	Fe	Si	Al
7.2	2.15	1.46	0.28	0.16	0.12	0.12	0.05	Rest

Heat treatment of the alloy was performed according to the following regimes:

a) Homogenization annealing at 460 ^{o}C/1h, quenching in water at room temperature, followed by precipitation hardening at 120 ^{o}C/24h (one-step aging, indicated in this paper as TA).

b)Homogenization annealing at 460 ^{o}C/1h, quenching in water at room temperature, precipitation hardening at 100 ^{o}C/5h, and then at 160 ^{o}C/5h (two-step aging, indicated in this paper as TB).

Tensile characteristics of the tested aluminium alloy after applied heat treatment regimes are given in Table 2.

Table 2 - Tensile characteristics of tested aluminium alloy

Thermal State	$R_{p0.2}$ (MPa)	R_m (MPa)	A_5 (%)
TA	560	620	10.5
TB	570	600	9.5

2.2. Scanning electron microscopy (SEM)

SEM-EDS analysis of aluminium alloy samples was performed using the scanning electron microscope JEOL JSM–6610LV coupled with INCA350 energy-dispersive analytic unit. The qualitative Electron Probe Micro Analysis (EPMA) was applied.

2.3. Measurements of electrical resistivity

Measurements were performed on TA and TB samples in accordance with standard ASTM B193 using a micro ohmmeter. Measured values of electrical resistivity (ρ) were recalculated into electrical conductivity ($\chi=1/\rho$), as well as into IACS % factor, using the following equation:

$$\text{IACS} = \frac{\chi}{\chi_{\text{Cu}}} \cdot 100\% \qquad (1)$$

where χ is electrical conductivity of the tested alloy, and χ_{Cu} is electrical conductivity of bare copper (58.34 MS m^{-1}).

2.4. Corrosion potential measurements

Corrosion potential measurements were performed in the 3.5 wt. % NaCl solution. The working electrodes (TA and TB samples) were degreased in ethanol and then placed in the electrochemical cell with a saturated calomel electrode (SCE) as a reference electrode. Changes in the corrosion potential were monitored at room temperature, in the presence of atmospheric air, during 60 min.

2.5. Polarization measurements

Cathodic and anodic polarization curves of aluminium alloy were obtained using the GAMRY Reference 600 Potentiostat/Galvanostat/ZRA in deaerated 3.5 wt. % NaCl at room temperature. A three-electrode cell arrangement was used in the experiments. The counter electrode was a platinum mesh with a surface area considerably greater than that of the working electrode. The reference electrode was the SCE. A potential sweep rate of 0.5 mV s^{-1} was applied after the stabile open circuit potential (OCP) was established (up to 30 min).

2.6. Electrochemical impedance spectroscopy measurements

Electrochemical impedance spectroscopy (EIS) measurements were performed in the 3.5 wt. % NaCl during 48 h. The same three-electrode cell arrangement was used as for polarization measurements. EIS data were acquired at the open circuit potential using the GAMRY Reference 600 Potentiostat/Galvanostat/ZRA. Impedance measurements were carried out over a frequency range of 100 kHz to 10 mHz using the 10 mV amplitude of sinusoidal voltage. The impedance spectra were analyzed by Gamry Elchem Analyst fitting procedure. In this case "Goodness of Fit" is the parameter which defines the precision of fitting.

3. RESULTS AND DISCUSSION

Tested aluminium alloy in TA and TB thermal state is characterized with appropriate microstructure, mechanical properties, electrical conductivity, corrosion resistance and electrochemical properties. Based on these indicators, the tendency of the alloy in different thermal state to localized corrosion was evaluated.

3.1. SEM-EDS analysis

Representative SEM microphotographs of aluminium alloy after one-step aging (TA) are shown in Fig. 1. Intermetallic compounds of Fe, Cu, Mn (usually with Al) are visible as bright fields in Fig. 1a, while intermetallic compounds of Mg, Si (also usually with Al) are visible as dark fields in Fig. 1b. Typical chemical composition of the intermetallic compounds (shown in Fig. 1) is presented in Table 3. Similar results were obtained for the alloy after two-step aging (TB).

Table 3 - Typical chemical composition of intermetallic compounds in Fig. 1a and b (at. %)

Element	O	Mg	Al	Si	Cr	Mn	Fe	Cu	Zn
Fig. 1a	1.61	0.38	83.5	0.00	0.13	1.32	8.98	2.32	1.72
Fig. 1b	1.90	16.9	65.3	13.7	0.00	0.00	0.00	0.43	1.78

Iron is the most common impurity in aluminium and its alloys. It has a high solubility in molten aluminium. However, the solubility of iron in the solid state is very low (~0.04 %) and therefore, most of the iron present in aluminium over this amount appears as an intermetallic second phase in combination with aluminium and often with other elements. Silicon, after iron, is the other impurity element of high level in commercial aluminium (0.01 to 0.15 %) [10].

a)

b)
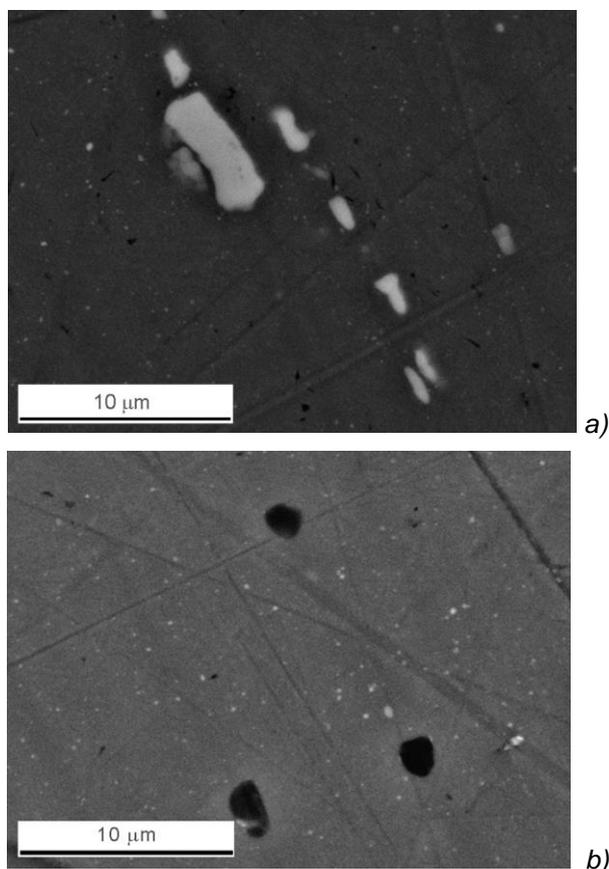
Figure 1 - SEM microphotographs of aluminium alloy after one-step aging (TA).

Taking into account that practically same intermetallic compounds are present within the tested alloy after one-step and after two-step aging it can be assumed that the composition of the solid solution (formed during aging process) has the greatest influence on the corrosion characteristic of this alloy. Values of corrosion potentials in 3.5 wt.

% NaCl for some intermetallic compounds can be found [14].

Microstructures of the alloy after one-step and after two-step aging are shown in Fig. 2, where hardening phases can be seen as bright spots. During one-step aging (TA), clusters of zinc atoms are formed at first, and after that GP zones that grow gradually and transform themselves into the half-coherent η' phase. It can be seen in Fig. 2a that precipitated hardening phases after one-step aging are smaller with regard to the hardening phases after two-step aging (Fig. 2b). It is possible that most of these phases are not visible in Fig. 2. The mixture of the η' phase and stabile η phase was formed during two-step aging (TB). Difference in size of the strengthening particles can be explained by reduced time of two-step aging (5h/100 °C + 5h/160 °C) compared to the time of standard one-step aging (120 °C/24h).

a)

b)
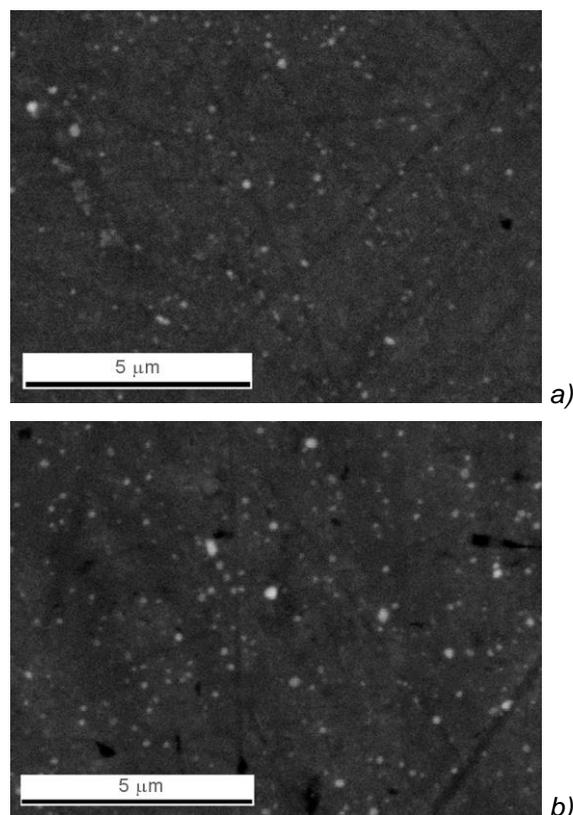
Figure 2 - SEM microphotographs of aluminium alloy: a) after one-step aging (TA), b) after two-step aging (TB).

3.2. Electrical resistivity

Electrical conductivity of the aluminium alloy in TA and TB thermal state is shown in Fig. 3. It can be seen that the alloy in TB state has greater conductivity (36.71 IACS %) than the alloy in TA state (32.56 IACS %). Electrical conductivity of the alloy immediately after homogenization annealing (T0 state) is 29.65 IACS %.

A supersaturated solid solution with a high concentration of vacancies was obtained after quenching. Fields of elastic strains around the vacancies caused dissipation of electrons which resulted in the lowest conductivity [15]. During the aging process, clusters of zinc atoms are formed at first. After that, GP zones are formed that grow gradually and transform themselves into the half-coherent phase η'. Elastic strains around the GP zones and the η' phase caused low values of electrical conductivity. With appearance of the stabile η phase during two-step aging (TB), elastic strains decrease and the alloy conductivity increases. With a prolonged time of aging, the conductivity still increases (approximately to 42 IACS % after 24 h) because of coarsening of formed precipitates. However, mechanical characteristics of the alloy (hardness) decrease, and resistance to exfoliation corrosion and SCC is reduced as well [4]. Resistance to SCC and exfoliation corrosion for aluminium alloys 7000 series can be evaluated according to values of electrical conductivity [16].
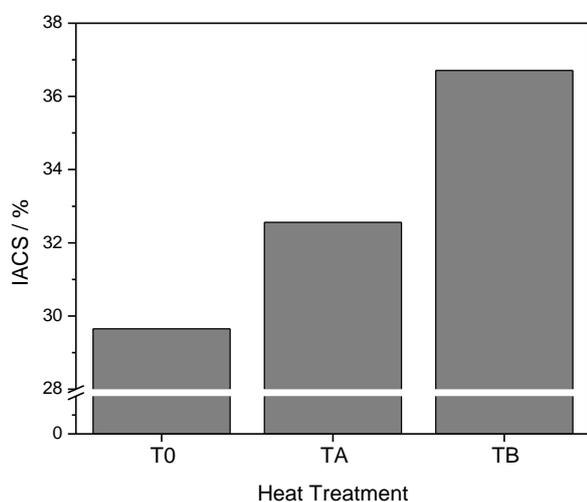
Figure 3 - Electrical conductivity (IACS % factor) of aluminium alloy after different heat treatment regimes.

3.3. Electrochemical properties

Corrosion potential of aluminium alloys depends on the content of alloying elements in the solid solution [9, 16]. As the content of alloying elements varies during the aging process (TA and TB), as a consequence of the precipitation of different phases, the corrosion potential was changed in a predictable way (Fig. 4). Results presented in Fig. 4 show that the corrosion potential is higher after two-step (TB) than after one-step aging (TA), that reduces thermodynamic driving force for corrosion processes to occur. This can be related to the kinetics of the precipitation hardening. The alloy in TA thermal state has a larger concentration of zinc (more negative) in the solid solution, which results in a more negative value of the corrosion potential (E_{corr} = −795 mV). In the case of TB thermal state (partially over-aged state), the enlargement of the strengthening precipitates occurs at the expense of impoverishment of the solid solution in zinc, magnesium and copper. This is in accordance with the measurements of electrical conductivity. In this case, the solid solution has a more positive corrosion potential (E_{corr} = −775 mV) due to depletion of solid solution in zinc and magnesium. Precipitates formed after two-step aging are electrically more positive than precipitates after one-step aging. Atoms of aluminium and copper replace to some extent atoms of zinc in $MgZn_2$ forming $Mg(AlCuZn)_2$. It was shown [17, 18] that the content of copper in this precipitate is approximately 20 at. %. Electrochemical and corrosion characteristics of different precipitates and intermetallic compounds existing in commercial precipitation-hardened aluminium alloys have been also studied [14, 17-23]. It was shown that electrochemical characteristics of intermetallic phases significantly affect corrosion current density of the solid solution in an aluminium alloy 7000 series [14]. It was also established that Cu content in the intermetallic compound $Mg(AlCuZn)_2$ greatly influenced corrosion behaviour of aluminium alloys 7000 series [17, 18].
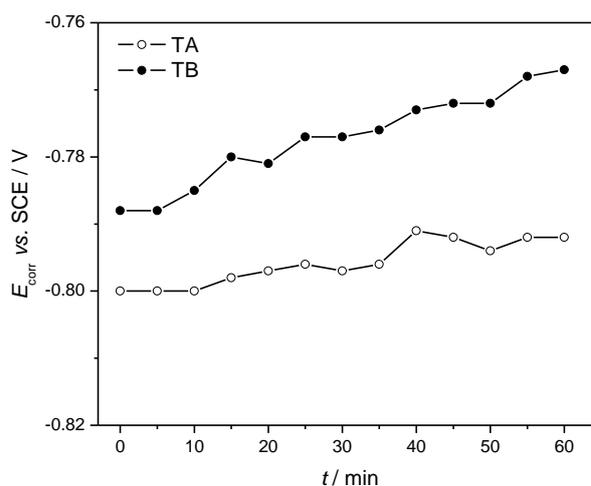
Figure 4 - Time dependence of E_{corr} for aluminium alloy in TA and TB state.

Polarization curves of aluminium alloy after one-step and two-step (TA) aging are shown in Fig. 5.

It can be seen that the alloy after two-step aging (TB) has a more positive value of the pitting potential ($E_{pit} = -775$ mV) with regard to the one-step aged alloy ($E_{pit} = -800$ mV). For the alloy in TB state anodic and cathodic curves are shifted to lower current densities and the corrosion current density is lower than for the alloy in the TA state.
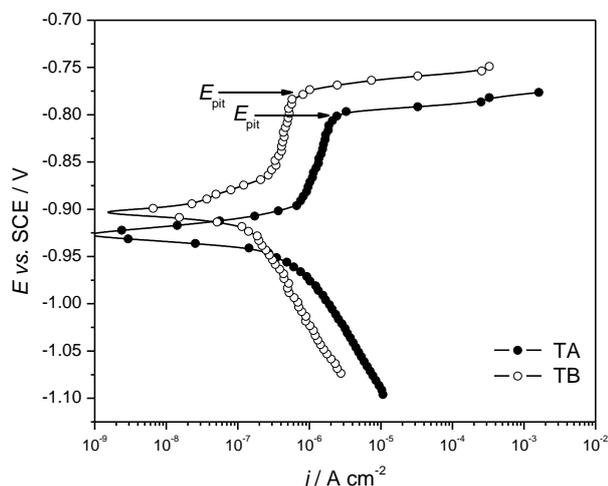
Figure 5 - Polarization curves of aluminium alloy in TA and TB state.

In aluminium alloys 7000 series, pitting occurs due to a local dissolution of the matrix or to dissolution of intermetallic compounds [24]. Intermetallic compounds containing Cu and Fe are cathodic with respect to the matrix and promote the matrix dissolution, while Mg-rich intermetallics (anodic to the matrix) dissolve preferentially. Alloy's behaviour after two-step aging could be explained by the difference in electrode potentials between intermetallic compounds and the solid solution as well as between the precipitates and the solid solution. It was noticed that two pitting potentials exist, with the appearance of the second pitting potential at current densities higher than 1 mA cm^{-2} [18, 25, 26]. The nature of these pitting potentials is considered in details [12, 25, 26]. In the 7000 series aluminium alloys with similar copper content as in the tested alloy, values of corrosion and pitting potential approaches each other in the presence of oxygen [18].

Corrosion and electrochemical characteristics of different aluminium alloys with and without protective coatings have been investigated by EIS technique [27-31]. In this work EIS measurements were performed in NaCl solution in the presence of atmospheric O$_2$, in order to compare corrosion behaviour of different thermal states of the tested alloy. The results of EIS measurements on the aluminium alloy in TA and TB state are presented in Nyquist plots in Fig. 6. The alloy in both thermal states shows one time constant semicircle after

one hour in 3.5 wt % NaCl. Polarization resistance, R_p (3.86 kΩ cm^2), of the alloy in TA state is lower (which corresponds to a higher value of corrosion rate) with regard to R_p (4.33 kΩ cm^2) of TB state. After 24 h, Warburg diffusion tail has appeared for the alloy in TA state. A similar diffusion tail has appeared later after 48 h, in the case of the alloy in TB state. However, the value of R_p is higher for TB state, which corresponds to a lower value of corrosion rate.
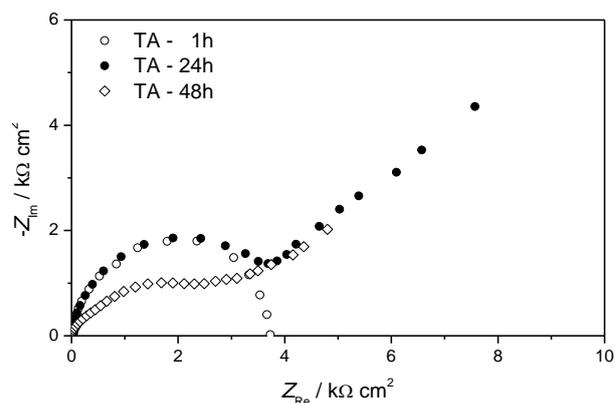
a)
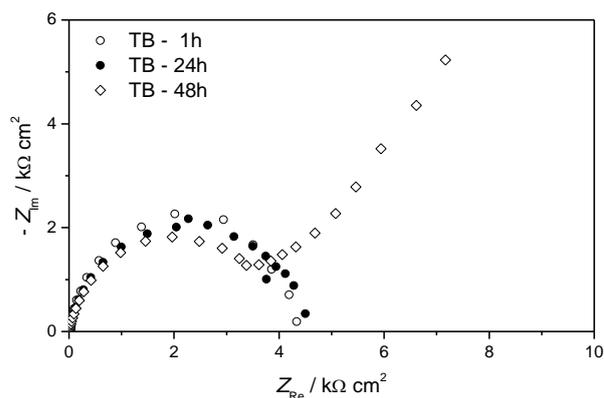
b)

Figure 6 - Nyquist plots of tested aluminium alloy in 3.5 wt. % NaCl, at room temperature: a) after one-step aging (TA), b) after two-step aging (TB).

A layer of dark corrosion products has been formed at the surface of aluminium alloy in TA and TB state, probably consisting of aluminium hyd-roxide Al(OH)$_3$ [18]. The nature and conditions of corrosion products formation on aluminium alloys 7000 series have been considered [18, 24]. It was shown that the Al(OH)$_3$ layer is about 120 nm thick and the corrosion products are amorphous [18]. Also, the presence of pits under a layer of corro-sion products, after the electrochemical tests in NaCl solution, was revealed [24].

Proposed equivalent electrical circuit (EEC) is shown in Fig. 7a. R_s is electrolyte resistance, R_p is

polarization resistance, C_{dl} is double-layer capacitance, and W represents diffusion processes (Warburg constant). The impedance data were well fitted by the proposed EEC, with corresponding values of the "Goodness of Fit" in the range $0.87 \cdot 10^{-3}$ – $7.4 \cdot 10^{-3}$. The quality of the fitting is illustrated in Fig. 7b, for TA state after 24 h of exposure to the NaCl solution. Solid line corresponds to the simulated curve obtained by fitting the elements of the proposed equivalent circuit.
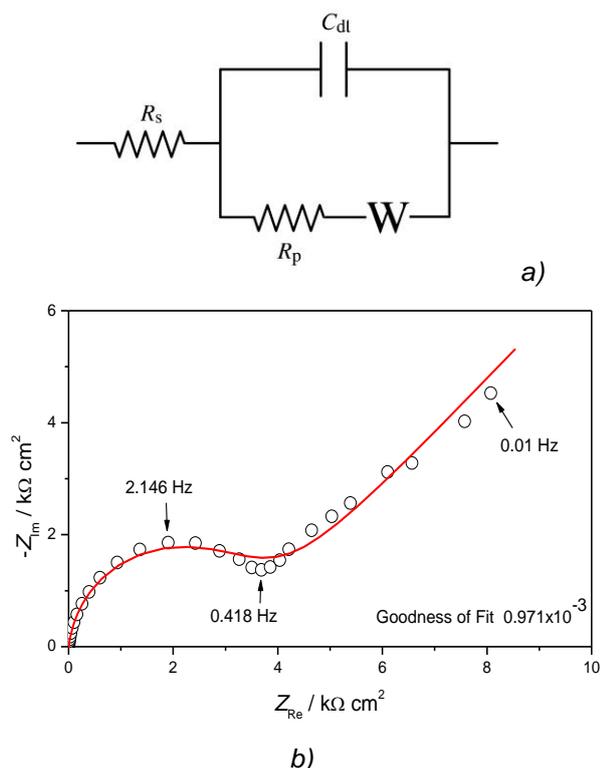
Figure 7 - a) Proposed equivalent electrical circuit and b) experimental data and fitted curve for aluminium alloy in TA state after 24h exposure in 3.5 wt. % NaCl, at room temperature.

The values of polarization resistance, R_p and double-layer capacitance, C_{dl} of the aluminium alloy at room temperature, as a function of exposure time in the 3.5 wt. % NaCl are given in Table 4.

Table 4 - Polarization resistance, R_p and double-layer capacitance, C_{dl}, of aluminium alloy in 3.5 wt. % NaCl at room temperature, after one-step aging (TA) and two-step aging (TB) for different exposure times

t / h	1	24	48
Rp (TA) / kΩ cm2	3.86	4.18	2.84
Rp (TB) / kΩ cm2	4.33	4.56	4.06
Cdl (TA) / μF cm-2	12.5	22.7	118.2
Cdl (TB) / μF cm-2	7.9	28.7	28.9

Significantly higher value of double-layer capacitance (C_{dl}) and lower value of polarization resistance (R_p) after 48h indicate the lower corrosion resistance of the alloy after one-step aging. However, it should be kept in mind that in exploitation of aluminium alloys electrochemical conditions on the tip of a pit or a stress corrosion crack (pH, concentration of chloride ions, voltage drop, etc.) are significantly different from electrochemical conditions at the alloy surface with a free access of electrolyte.

4. CONCLUSIONS

Corrosion resistance of a high strength aluminium alloy 7000 series (Al-Zn-Mg-Cu) was investigated. The alloy was subjected to the standard one-step aging process as well as to a new two-step aging process. It was shown that same intermetallic compounds are present within the alloy after one-step and after two-step aging which indicates great influence of chemical composition of the solid solution on the corrosion behaviour of the alloy. Electrical conductivity of the aluminium alloy after two-step aging is higher than those of the alloy after one-step aging and after homogenization annealing. Corrosion potential of the alloy after two-step aging is more positive, compared to that of the alloy after one-step aging because of different distribution of alloying elements (Zn, Mg, Cu) in the solid solution and in the precipitated phases. Anodic and cathodic polarization curves of the alloy after two-step aging are shifted to the lower current densities and the corrosion current density (j_{corr}) is lower than for the alloy in the TA state, indicating lower electrochemical activity. The pitting potential value of the alloy after two-step aging is more positive than the value after one-step aging, which means better resistance to pitting corrosion of the aluminium alloy in the TB state. Higher resistance to localized corrosion of the alloy after two-step aging (higher values of R_p and lower values of C_{dl}) in respect to the alloy after one-step aging was proved.

REFERENCES

[1] Scamans G.M., Birbilis N., Buchheit R.G., Corrosion of Aluminum and its Alloys, Comprehensive Corrosion, in Shreir's Corrosion, Fourth Edition, Oxford: Academic Press, 2010, p. 1974.

[2] Kaufman J.G., Corrosion of Aluminum and Aluminum Alloys, ASM Handbook, Volume 13B: Corrosion: Materials, Ohio: ASM International, 2005, p. 95.

[3] Speidel M.O. (1975) Stress Corosion Cracking of Aluminum Alloys, Metallurgical Transactions A, 6A (4), pp. 631-651.

[4] Thompson A.W., Bernstein I.M. (1980) The Role of Metallurgical Variables in Hydrogen-assisted Environmental Fracture, Advances in Corrosion Science and Technology, Vol 7, Eds. Fontana M.G., and Staehle R.W., New York: Plenum Press, p. 53.

[5] Kannan M.B., Srinivasan P.B., Raja V.S. (2011) Stress corrosion cracking (SCC) of aluminium alloys, in Stress corrosion cracking, Theory and practice, Edited by: Raja V.S., and Shoi T., Oxford: Woodhead Publishing, p. 307.

[6] Jegdić V.B. (2003) Behavior of Stress Corrosion Crack in a High-Strength Aluminum Alloys Structure, Scientific-Technical Review, 53 (4), pp. 19-24.

[7] Peng G.S., Chen K.H., Chen S.Y., Fang H.C. (2012) Influence of dual retrogression and re-aging temper on microstructure, strength and exfoliation corrosion behavior of Al–Zn–Mg–Cu alloy, Transactions of Nonferrous Metals Society of China, 22 (4), pp. 803-809.

[8] Ralston K.D., Birbilis N., Weyland M., Hutchinson C.R. (2010) The effect of precipitate size on the yield strength-pitting corrosion correlation in Al–Cu–Mg alloys, Acta Materialia, 58 (18), pp. 5941–5948.

[9] Summerson T.J., Sprowls D.O. (1986) Corrosion Behavior of Aluminum Alloys, Vol. III, Conference Proceedings, Aluminum Alloys-Physical and Mechanical Properties, Virginia, pp. 1576-1662.

[10] Hatch J.E. (1984) Aluminum: Properties and Physical Metallurgy, Ohio: American Society for Metals, p. 134.

[11] Sha G., Cerezo A. (2004) Early-stage precipitation in Al–Zn–Mg–Cu alloy (7050), Acta Materialia, 52 (15), pp. 4503–4516.

[12] Kappes M., Kovarik L., Mills M.J., Frenkel G.S., Miller M.K. (2008) Usefulness of Ultrahigh Resolution Microstructural Studies for Understanding Localized Corrosion Behavior of Al Alloys, Journal of the Electrochemical Society, 155 (8), C437-C443.

[13] Jegdić V.B., Bobić M.B., Pavlović K.M., Alil B.A., Putić S.S., Stress Corrosion Cracking Resistance of Aluminium Alloy 7000 Series After New Two-Step Aging, Chemical Industry and Chemical Engineering Quarterly, submitted.

[14] Birbilis N., Buchheit R.G. (2005) Electrochemical Characteristics of Intermetallic Phases in Aluminum Alloys, An Experimental Survey and Discussion,

Journal of the Electrochemical Society, 152 (4), B140-B151.

[15] Novikov I.I., Theory of heat treatment of metals, Moscow: Mir Publishers, 1978, p. 298.

[16] Davis J.R., Corrosion of Aluminum and Aluminum Alloys, Ohio: ASM International, 1999, p. 99.

[17] Ramgopal T., Schmutz P., Frankel G.S. (2001) Electrochemical Behavior of Thin Film Analogs of $Mg(Zn,Cu,Al)_2$,. Journal of the Electrochemical Society, 148 (9), B348-B356.

[18] Meng Q., Frankel G.S. (2004) Effect of Cu Content on Corrosion Behavior of 7xxx Series Aluminum Alloys, Journal of the Electrochemical Society, 151 (5), B271-B283.

[19] Frankel G.S. (1998) Pitting Corrosion of Metals, A Review of the Critical Factors, Journal of the Electrochemical Society, 145 (6), pp. 2186-2198.

[20] Marlaud T., Deschamps A., Bley F., Lefebvre W., Baroux B. (2010) Influence of alloy composition and heat treatment on precipitate composition in Al–Zn–Mg–Cu alloys, Acta Materialia, 58 (1), pp. 248–260.

[21] Birbilis N., Buchheit R.G. (2008) Investigation and Discussion of Characteristics for Intermetallic Phases Common to Aluminum Alloys as a Function of Solution pH, Journal of the Electrochemical Society, 155 (3), C117-C126.

[22] Xu D.K., Birbilis N., Lashansky D., Rometsch P.A., Muddle B.C. (2011) Effect of solution treatment on the corrosion behaviour of aluminium alloy AA7150: Optimisation for corrosion resistance, Corrosion Science, 53 (1), pp. 217–225.

[23] Knight S.P., Birbilis N., Muddle B.C., Trueman A.R., Lynch S.P. (2010) Correlations between inter-granular stress corrosion cracking, grain-boundary microchemistry, and grain-boundary electrochemistry for Al–Zn–Mg–Cu alloys, Corrosion Science, 52 (12), pp. 4073–4080.

[24] Andreatta F., Terryn H., De Wit J.H.W. (2004) Corrosion behaviour of different tempers of AA7075 aluminium alloy, Electrochimica Acta, 49 (7), pp. 2851–2862.

[25] Zhao Z., Frankel G.S. (2007) On the first breakdown in AA7075-T6, Corrosion Science, 49 (7), pp. 3064–3088.

[26] Zhao Z., Frankel G.S. (2007) The effect of temper on the first breakdown in AA7075, Corrosion Science, 49 (7), pp. 3089–3111.

[27] Bajat B.J., Popić P.J., Mišković-Stanković B.V. (2010) The influence of aluminium surface pretreatment on the corrosion stability and adhesion of powder polyester coating, Progres in Organic Coatings, 69 (4), pp. 316-321.

[28] Lazarević Z.Ž., Mišković-Stanković B.V., Kačarević-Popović Z., Dražić M.D. (2005) Determination of the protective properties of electrodeposited organic epoxy coatings on aluminium and modified aluminium surfaces, Corrosion Science, 47 (3), pp. 823-834.

[29] Živković S. Lj., Jegdić V.B., Popić P.J., Bajat B.J., Mišković-Stanković B.V. (2013) The influence of Ce-based coatings as pretreatments on corrosion stability of top powder polyester coating on AA6060, Progress in Organic Coatings, 76 (10), pp. 1387–1395.

[30] Bajat B.J., Milošev I., Jovanović Ž., Janjić-Heinemann R.M., Dimitrijević M., Mišković-Stanković B.V. (2010) Corrosion protection of aluminium pretreated by vinyltriethoxysilane in sodium chloride solution, Corrosion Science, 52 (3), pp. 1060-1069.

[31] Venugopal A., Panda R., Manwatkar S., Sreekumar K., Krishna R.L., Sundararajan G. (2012) Effect of micro arc oxidation treatment on localized corrosion behaviour of AA7075 aluminum alloy in 3.5% NaCl solution, Transactions of Nonferrous Metals Society of China, 22 (3), pp. 700-710.

IZVOD

OTPORNOST PREMA KOROZIJI ALUMINIJUMSKE LEGURE SERIJE 7000 POSLE NOVOG DVOSTEPENOG TERMIČKOG TALOŽENJA

Otpornost prema koroziji aluminijumske legure serije 7000 ispitivana je primenom različitih elektrohemijskih metoda. Legura je bila podvrgnuta jednostepenom i novom dvostepenom termičkom taloženju. Polarizaciona merenja u 3,5 mas.% NaCl su pokazala da legura posle dvostepenog termičkog taloženja ima pozitivniju vrednost potencijala pitinga (E_{pit}) i veću otpornost prema koroziji. Spektroskopija elektrohemijske impedancije (SEI) je takođe pokazala da legura posle dvostepenog termičkog taloženja ima bolju otpornost prema koroziji (veću vrednost polarizacione otpornosti, R_p i manju vrednost kapacitivnosti dvojnog sloja, C_{dl}) u poređenju sa legurom posle jednostepenog termičkog taloženja.

Ključne reči: *aluminijumske legure, termičko taloženje, korozija, elektrohemijske metode*